

Neutron capture by ^{31}P

R. L. Macklin

Oak Ridge National Laboratory, Oak Ridge, Tennessee 37831

S. F. Mughabghab

Brookhaven National Laboratory, Upton, New York 11973

(Received 11 March 1985)

Resonance parameters for $^{31}\text{P}+n$ were determined, largely from (n,γ) cross-section data measured by time of flight. The energy range investigated extended from 2.6 to 500 keV, with the lowest energy resonance found at 26.75 keV. The 30-keV stellar reaction rate is dominated by this resonance, giving 1.74 ± 0.09 mb for a temperature $kT=30$ keV. The thermal capture data are examined within the framework of the direct reaction mechanism.

INTRODUCTION

Little work has been reported on neutron resonances of ^{31}P since the Van de Graaff transmission studies in the 1950's and 1960's at Duke,¹ MIT,² and Bartol³ which found no resonances below 90 keV. Neutron capture spectra at the 26.75 keV resonance have been reported by Nystroem *et al.*⁴ Most of the narrow structure seen with 2-keV resolution² is found in the present capture cross section data up to 500 keV.

EXPERIMENT

A 6.77 ± 0.07 g sample of reagent grade red phosphorus powder was pressed to a 28.6.-mm-diameter, 6-mm-thick disc. Despite a little crumbling at the edges, it survived mounting in the 40-m vacuum flight path at the Oak Ridge Electron Linear Accelerator (ORELA). The uncertainty in mass was derived from weighings before and after the neutron-capture measurement. The nominal ORELA time-of-flight resolution was 0.12 ns/m, but the

experimental resolution function was compounded from the spread in moderator slowing-down time and electronic-timing jitter. It also showed some exponential tailing as seen in the narrowest resonances.

Capture gamma rays were recorded by a pair of nonhydrogenous liquid scintillators flanking the sample just outside the collimated beam.⁵ Pulse-height weighting was used to give an unbiased estimate of the gamma-ray energy release. Division by the known excitation energy of the compound nucleus gave the number of neutrons captured as a function of time of flight or neutron energy. A calculated 4.0% loss of gamma-ray energy, primarily to Compton scattering in the phosphorus, was included in the calculation.

The neutron flux was determined from a thin ^6Li glass scintillator in the beam ~ 0.4 m in front of the sample. The absolute detection efficiency for neutron capture was determined at 4.9 eV by the saturated resonance peak technique. The relative efficiency of the neutron monitor versus energy above 70 keV had been calibrated with a $^{235}\text{U}(n,f)$ fission counter,⁶ assuming the ENDF/B-V cross

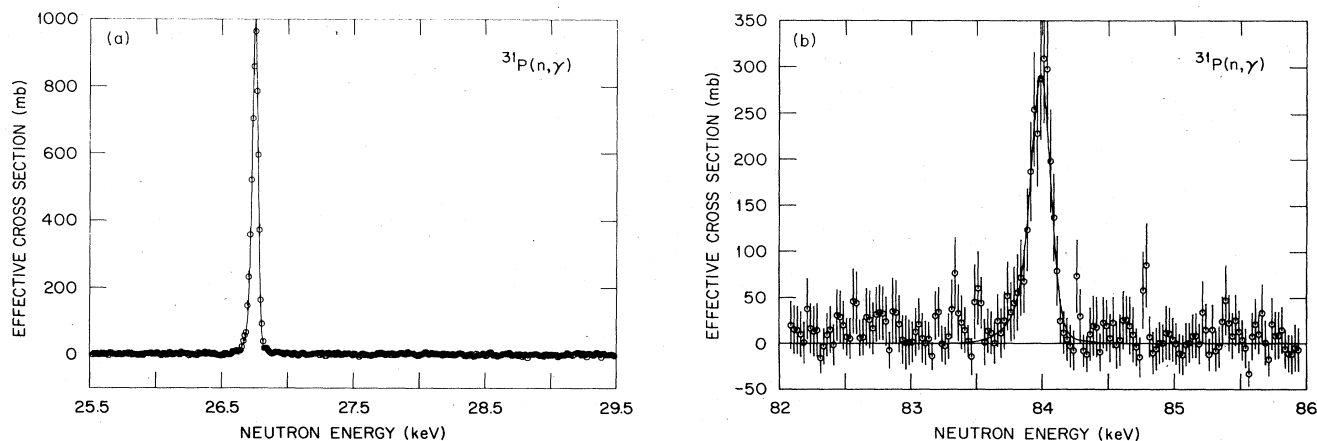


FIG. 1. The $^{31}\text{P}(n,\gamma)$ resonance yield for the 0.01025-atom/b sample. Statistical counting uncertainties are shown with the data points. Solid lines correspond to the least-squares-adjusted parameters given in Table I.

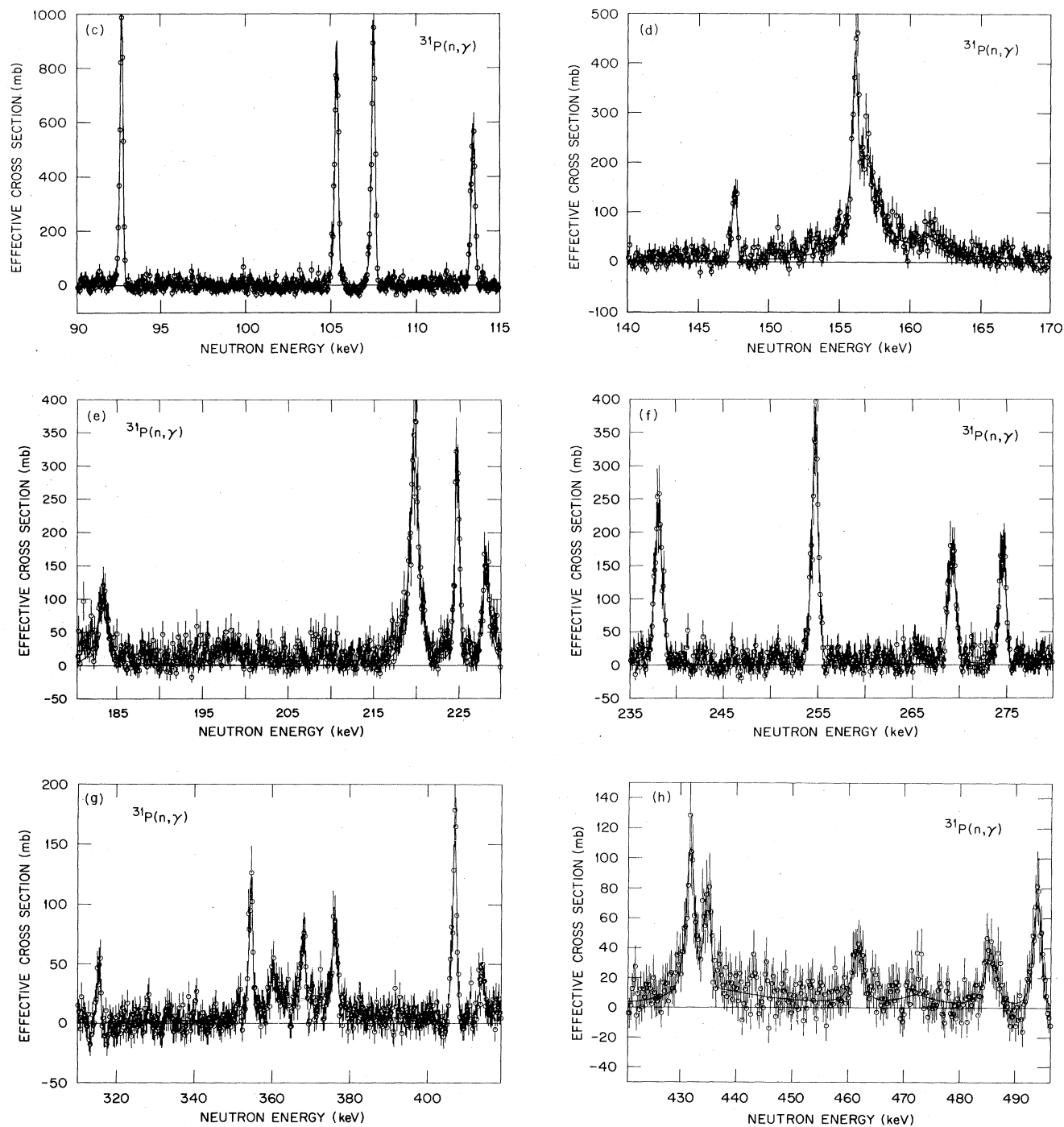


FIG. 1. (Continued).

section.

Peaks in the cross section were fitted with resonance parameters by nonlinear least-squares adjustment as shown by the solid lines in Fig. 1. Possible additional peaks may be present but are not considered well enough defined to warrant a claim of resonance identification without additional evidence. The resolution function is

well enough known to rule out narrower peaks as, for example, near 84.8 keV and the uncertainty in the background level makes small broader bumps such as that near 82.8 keV questionable. The fitting code includes the calculation of Doppler broadening, resonance self-protection, and scattering before capture within the sample convoluted with the experimental resolution function.

DISCUSSION

The fitted resonance parameters are listed in Table I. The peak areas give a quantity $g\Gamma_\gamma\Gamma_n/\Gamma$ which is probably dominated by the radiation width with a statistical weight $g=0.75$ in the majority of cases. When the total width of a resonance was between 0.2 and 100 times the resolution width, it could also be determined. Still broader resonance widths and positions were estimated from the total cross section.² A peak at 472 keV with width 6.7 keV was included in the fitting, but the adjustment did not give a statistically significant capture area. For the still broader peaks at 367 and 436 keV, most of the observed area is attributable to neutrons scattered by the sample and captured in the detector, phototubes, and mountings. For the narrower resonances a correction for this effect was made as noted in Table I.

A plot of the capture kernels $g\Gamma_\gamma\Gamma_n/\Gamma$ (not shown) did not give evidence of clustering which could be associated with resonance spin quantum numbers or orbital angular momentum. For heavy nuclei where radiation widths are nearly constant from resonance to resonance, this method could be used to assign quantum numbers. In lighter odd nuclei such as ^{27}Al and ^{23}Na where quantum numbers have been assigned, variations of Γ_γ exceeding a factor of 5 are common.⁷ Thus, the neutron resonances of ^{31}P are probably similar in that respect.

Because the peak of the $2p$ -wave neutron strength function is located at about mass number 24, where the s -wave neutron strength function has a minimum value,⁷ it is ex-

pected that most of the presently observed resonances are due to p -wave neutrons. The resonance at 156.9 keV reported¹ in previous total cross-section measurements is identified as due to s -wave neutrons because of the presence of an interference minimum at the low-energy side of the resonance. If then we assume that all the other resonances are formed by p -wave neutrons, we derive, by the method of the staircase plot (Fig. 2), a p -wave neutron strength function $S^1=(0.51\pm 0.15)\times 10^{-4}$, which is in good agreement with the systematics in this mass region.⁷

The observed resonances do not appear to account for more than 2 mb of the thermal capture cross section. Furthermore, a large and significant correlation coefficient between reduced primary γ -ray intensities and the (d,p) spectroscopic factors of the final p states was previously reported⁸ for the $^{31}\text{P}(n,\gamma)^{32}\text{P}$ reaction at thermal neutron energy. This correlation coefficient is maximized for a unit power of the γ -ray energy. These criteria signify a dominance of the direct capture mechanism. Therefore, it is of great interest to calculate the partial radiative capture cross sections in the framework of the direct reaction mechanism⁹ in order to compare with the thermal data.

The direct radiative cross section due to an s -wave neutron which is captured by a target of spin I into a p -orbital final state is given⁷ by

$$\sigma_{\gamma f} = \sum_i \sigma_{if} S_{if}^2, \quad (1)$$

where

TABLE I. $^{31}\text{P}(n,\gamma)$ resonance parameters.

E_{res} (lab) (keV)	$g\Gamma_\gamma\Gamma_n/\Gamma^a$ (meV)	Γ^b (keV)	E_{res} (lab) (keV)	$g\Gamma_\gamma\Gamma_n/\Gamma$ (meV)	Γ (keV)
26.75	455±5	<0.003	269.3	1310±90	0.31±0.03
84.00	141±8	<0.03	274.6	1110±70	<0.13
92.74	575±20	<0.03	315.6	450±50	<0.15
105.11	649±25	<0.04	354.6	1290±90	<0.18
107.5	727±28	<0.04	360.5	740±120	1.2±0.3
113.4	488±24	<0.04	(367)		(25)
147.6	238±21	<0.06	368.0	950±100	0.46±0.08
156.1	497±44	<0.06	376.2	1340±130	0.64±0.10
156.9	2500±210	2.03±0.14	407.0	2190±120	<0.2
161.5	350±90	1.7±0.6	414.2	1000±115	1.2±0.2
183.5	915±100	1.3±0.2	431.8	2190±180	0.58±0.07
219.8	3100±140	0.911±0.07	434.9	1180±130	<0.2
224.8	1170±80	<0.10	(436)		(20)
228.2	1160±90	0.65±0.07	462.0	1280±160	1.3±0.3
238.2	1630±90	0.41±0.03	485.7 ^c	1350±170	1.3±0.3
254.8	2150±120	0.21±0.02	494.1	1700±160	<0.3

^aThe indicated uncertainties are statistical standard deviations combined in quadrature with a 50% uncertainty in the scattered neutron sensitivity correction, which last was 21% for the 161.5-keV resonance and less than 15% for all others. Systematic uncertainties are estimated at 5%.

^bThe indicated uncertainty in width is the statistical standard deviation found in least squares adjustment to the data as shown in the figures. Parenthetic values were not adjusted by least squares.

^cAn additional resonance at 472 keV with a 6.7-keV width was included in the adjustment, but the capture area found was not statistically significant [see Fig. 1(h)].

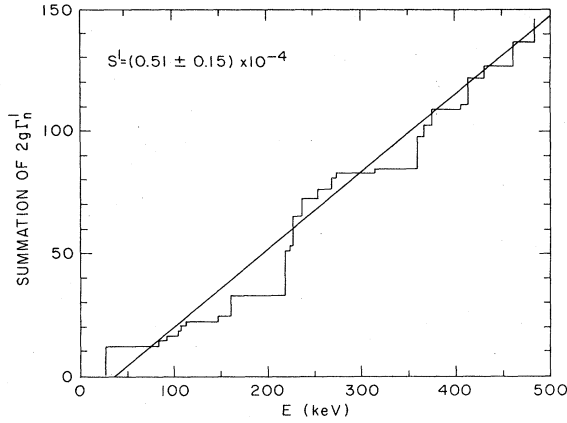


FIG. 2. Cumulative p -wave strength as a function of neutron energy for $^{31}\text{P} + n$. The slope of the straight line corresponds to the derived strength function.

$$S_{if}^2 = (2J_i + 1)(2J_f + 1) \left[2 \begin{Bmatrix} \frac{3}{2} & \frac{1}{2} & 1 \\ J_i & J_f & I \end{Bmatrix} S_{3/2} - \sqrt{2} \begin{Bmatrix} \frac{1}{2} & \frac{1}{2} & 1 \\ J_i & J_f & I \end{Bmatrix} S_{1/2} \right]^2, \quad (2)$$

$$\sigma_{if} = \frac{0.062}{R\sqrt{E_n}} \left[\frac{Z}{A} \right]^2 \frac{y_f^2}{6(2I+1)} \left[\frac{y_f+3}{y_f+1} \right]^2 \times \left[1 + \frac{R_i - a_{si}}{R_i} y_f \frac{y_f+2}{y_f+3} \right]^2, \quad (3)$$

$$y_f^2 = \frac{2mE_\gamma R_i^2}{h^2}, \quad (4)$$

where $S_{3/2}$ and $S_{1/2}$ are, respectively, the $P_{3/2}$ and $P_{1/2}$ (d,p) spectroscopic amplitudes of the final states; J_i and J_f are the initial and final spins, respectively; R_i is the interaction radius; and a_{si} is the coherent scattering length. The summation is carried out over the two channel spins $i = I + \frac{1}{2}$ and $I - \frac{1}{2}$. These two channel spins will later be designated by the + and - signs, respectively. The curly brackets represent Wigner's $6j$ coefficients.

It is instructive to present here an expression for the channel spin admixture coefficient, α , defined as the ratio of the capture cross section due to channel spin $I + \frac{1}{2}$ to that of the total capture cross section. For the present case of a ^{31}P target with spin $I = \frac{1}{2}$ and for a final spin $J_f = 1$ of ^{32}P and for the special case where $a_+ = a_-$, one obtains from Eqs. (1)–(3)

$$\alpha = \frac{(S_{3/2} - \sqrt{2}S_{1/2})^2}{3(S_{3/2}^2 + S_{1/2}^2)}. \quad (5)$$

Note that $\alpha = \frac{1}{3}$ or $\frac{2}{3}$ when the final 1^- states of ^{32}P are characterized as either a pure $P_{3/2}$ or $P_{1/2}$ single particle state, respectively.

To carry out the calculations of the partial capture

cross sections requires the coherent and incoherent scattering lengths, as well as the (d,p) spectroscopic factors. The coherent scattering length was accurately measured,¹⁰ but only an upper limit of 0.8 fm was reported¹¹ for the incoherent scattering length, i.e., $|a_+ - a_-| \leq 0.8$ fm. However, additional information on the latter can be deduced from an examination of the measured¹² channel admixture coefficients, α , for the final states at $E_x = 4036$ keV ($\alpha = 0.32 \pm 0.02$) and $E_x = 5776$ keV ($\alpha = 0.57 \pm 0.04$), which, according to Eq. (5) and the discussion following it, strongly suggest that $a_+ = a_-$. The (d,p) spectroscopic factors of the final p states are based on the available DWBA analysis¹³ for the states at excitation energies of 3264, 4007, and 4036 keV and the results¹⁴ of the Butler-Born approximation for the remainder of the states, with the latter values normalized to the former. As a starting point, an interaction radius of 4.24 fm was used in the calculations. However, the resulting predictions of the cross sections are much smaller than the measured values. By a χ^2 minimization procedure, an interaction radius of 5.1 ± 0.2 fm was found which departs from the value obtained from the prescription $R = 1.35A^{1/3}$. The results of the computations are summarized in the seventh column of Table II and are compared with the experimental data in the sixth column. The latter are obtained by a weighted average of the reported measurements^{15,16} and are based on a thermal capture cross section of 172 ± 6 mb. An uncertainty of 10–15% can be placed on the calculations, which is essentially a reflection of the uncertainty of the spectroscopic factors. As can be seen from Table II, within the limits of the errors, there is reasonably good agreement between measured and calculated values, which indicates that the compound nucleus contribution is quite small.

It is of interest to estimate the centroid energies of the single particle $P_{1/2}$ and $P_{3/2}$ states in ^{32}P . With the data of Table II, we obtain $E_x(P_{3/2}) = 4.52$ MeV and $E_x(P_{1/2}) = 5.85$ MeV. The latter value is derived on the assumption that all the reported p states above 5.509 MeV are of $P_{1/2}$ single-particle character. This information yields a splitting of 1.33 MeV for the $P_{3/2}$ and $P_{1/2}$ single particle states in ^{32}P . Furthermore, the centroid energy of the single-particle p state is determined to be at an excitation energy of 5.05 MeV; i.e., it is bound by 2.89 MeV, which accounts for the relatively low value of the p -wave neutron strength function of $^{31}\text{P} + n$ near the neutron

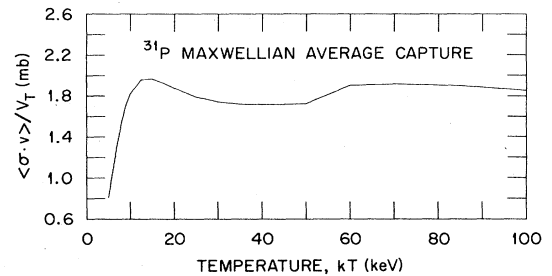


FIG. 3. Average neutron capture cross sections of ^{31}P for stellar temperatures from $kT = 5$ to 100 keV. The absence of low-energy resonances causes the average to decrease sharply below 10 keV.

TABLE II. Comparison between measurements and predictions of partial radiative cross sections for $^{31}\text{P}(n,\gamma)^{32}\text{P}$ at thermal neutron energy.

E_γ (keV)	E_x (keV)	J^π	j	$(2J_f+1)S_{\text{dp}}$	Expt. ^a	$\sigma_{\gamma f}$ (mb) Theory ^b	Theory ^c
4670	3264	2 ⁻	$P_{3/2}$	1.1	22.9±1.9	26.0	11.4
3927	4007	2 ⁻	$P_{3/2}$	0.33	6.5±1.0	6.8	3.2
3898	4036	1 ⁻	$P_{3/2}$	1.3	28.6±2.0	26.7	13.9
3271	4663	2 ⁻	$P_{3/2}$	0.40 ^d	8.9±0.6	7.2	3.7
3056	4878	1 ⁻	$P_{3/2}$	0.42 ^d	10.0±0.9	7.1	3.7
2584	5350	2 ⁻	$P_{3/2}$	0.72	8.8±0.9	10.8	5.9
2425	5509			0.24	3.8±0.7	3.4	1.9
2158	5776	1 ⁻	$P_{1/2}$	0.74	11.7±1.0	9.7	5.6
1874	6060			0.26 ^d	3.4±1.0	3.1	1.8
1739	6195			0.20 ^d	4.3±2.1	2.2	1.4

^aWeighted averages of the γ -ray intensities of Refs. 15–17 combined with $\sigma_\gamma^0=172\pm 6$ mb.

^bPredictions of channel capture for an interaction radius of 5.1 fm.

^cPredictions of channel capture for a conventional $1.35A^{1/3}$ interaction radius of 4.24 fm.

^dSpectroscopic factors are not well determined since angular distribution data at forward angles are not measured (see Ref. 14).

threshold.

The neutron capture rate in the interior of a star has been calculated for a series of stellar temperatures. At the conventional nucleosynthesis temperature $kT=30$ keV, the average velocity weighted cross section is 1.74 ± 0.09 mb, which is dominated by the resonance at 26.75 keV (Fig. 3).

The estimated overall systematic uncertainty in capture is $\sim 5\%$ and in resonance energy is $<0.05\%$ for the narrower well-defined peaks.

CONCLUSIONS

Resonance parameters were extracted from the $^{31}\text{P}(n,\gamma)^{32}\text{P}$ reaction in the energy region from 26 to 494 keV. A p -wave neutron strength function of

$S^1=(0.51\pm 0.15)\times 10^{-4}$ is deduced, which is in good agreement with the systematics in this mass region. The average weighted cross section for temperature $kT=30$ keV is calculated to be 1.74 ± 0.09 mb. The thermal capture data are examined and interpreted in terms of the direct capture mechanism.

ACKNOWLEDGMENTS

J. H. Oliver of the Oak Ridge National Laboratory prepared the pressed powder sample, and the ORELA operators and engineers provided pulsed neutrons for the experiment. The research was sponsored by the U. S. Department of Energy, Office of Basic Energy Sciences, under contract DE-AC05-84OR21400 with the Martin Marietta Energy Systems, Inc.

¹J. R. Patterson, H. W. Newson, and E. Mertzbacher, Phys. Rev. **99**, 1625 (1965), and private communication.

²K. F. Hansen, R. M. Krehn, and C. Goodman, Phys. Rev. **92**, 652 (1953).

³S. C. Snowdon and W. D. Whitehead, Phys. Rev. **90**, 615 (1953).

⁴G. Nystroem, B. Lundberg, and I. Bergqvist, Phys. Scr. **4**, 95 (1971).

⁵H. Beer and R. L. Macklin, Phys. Rev. C **26**, 1404 (1982), and references therein for a thorough discussion of techniques, corrections, and uncertainties.

⁶R. L. Macklin, R. W. Ingle, and J. Halperin, Nucl. Sci. Eng. **71**, 205 (1979).

⁷S. F. Mughabghab, *Neutron Cross Sections* (Academic, New York, 1984), Vol. 1B.

⁸S. F. Mughabghab, in *Proceedings of the Second International Symposium on Neutron Capture Gamma Ray Spectroscopy*

and Related Topics, Petten, 1974 (Reactor Centrum Nederland, Petten, 1975), p. 53, and references therein.

⁹A. M. Lane and J. E. Lynn, Nucl. Phys. **17**, 563 (1960).

¹⁰L. Koester, K. Knopf, and W. Waschkowski, Z. Phys. A **277**, 77 (1976).

¹¹H. Glattli and J. Coustham, J. Phys. (Paris) **44**, 957 (1983).

¹²J. De Boer, K. Abrahams, J. Kopecky, and P. M. Endt, Nucl. Phys. A **352**, 125 (1981).

¹³J. J. M. Van Gasteren, A. J. L. Verhage, and J. F. Van der Veen, Nucl. Phys. A **210**, 29 (1973).

¹⁴T. Holtebeck, Nucl. Phys. **37**, 353 (1962).

¹⁵H. Lycklama and T. J. Kennett, Can. J. Phys. **45**, 3039 (1967).

¹⁶G. Van Middlekoop, Nucl. Phys. A **97**, 209 (1967).

¹⁷N. C. Rasmussen, V. J. Orphan, T. L. Harper, J. Cunningham, and S. A. Ali, Gulf General Atomic Report GA-10248, 1970.